South Eastern Australian Climate initiative

Final report for **Project 1.4.1**

Application of the Bureau of Meteorology downscaling technique to reanalyses: implications for the attribution of observed climate change

Principal Investigator:
Dr. Bertrand Timbal, Centre for Australian Weather and Climate Research (CAWCR)
B.Timbal@bom.gov.au

Co-Author:

Elodie Fernandez (CAWCR)

CSIRO Land and Water
Ph: 02 6246 5617
seaci@csiro.au
http://www.seaci.org

Australian Government
Department of Climate Change
Bureau of Meteorology

MURRAY–DARLING BASIN AUTHORITY

State Government Victoria Department of Sustainability and Environment

National Research FLAGSHIPS Water for a Healthy Country CSIRO

Initial Project objectives

- Use the Bureau of Meteorology (BoM) Statistical Downscaling Model (SDM) developed as part of project 1.3.1 to study the relationship between observed local changes and large-scale changes during the 2nd half of the 20th Century.

- Investigate the individual role of the predictors selected in project 1.3.1 to explain the climatic trends (warming trend and drying trend) observed during the last decade.

- Ensure the SDM is applicable to climate model simulations of the 20th Century (i.e. is likely to increase the regional climate change signal by relating it to large-scale changes) in order to conduct attribution studies (project 1.5.1).

Proposed methodology

- The optimised SDM will be applied to the joint NCEP/NCAR re-analyses from 1958 to 2006 in order to investigate the large-scale predictors which relate to the observed changes. The focus is on the predictors found skilful during project 1.3.1.

- The technique will be applied separately to rainfall, daily temperature extreme (max and min) and humidity datasets (dew point temperature max and min and pan-evaporation).

- The seasonality of the changes will be investigated with a focus on the autumn to early winter rainfall decline.

- The SEACI relevant dataset assembled during project 1.1.1 will be used and separated in sub-regions according to climate entities defined on project 1.3.1.

Summary of the findings

- The BoM SDM was found able to reproduce a large part (60 to 80 per cent) of the observed rainfall decline in autumn. In other seasons, local rainfall trends, either positive or negative, are generally well reproduced in term of magnitude and spatial structures.

- Observed temperature trends (always positive with the exception of T_{min} in autumn) are well captured. The spatial structure is relatively well reproduced but the magnitude is consistently underestimated. Most of this underestimation is due to the reduced interannual variability of the reconstructed series and can be dealt with by "normalising" the trends (i.e. factoring in the underestimation of the inter-annual variability).

- Mean sea level pressure (MSLP) is the most important single predictor in explaining rainfall trends. However, when large rainfall trends are observed, MSLP alone is not sufficient and additional predictors (in particular moisture variable such as specific humidity at 850 hPa) ensure that optimised combinations of predictors better match the observed trends.

- In contrast to rainfall, MSLP, as a single predictor, explains very little of the observed temperature trends. Tropospheric temperature (at 850 hPa) is often the most important predictor in explaining local warming but tends in some cases to produce larger trends than observed (e.g. T_{min} in autumn). In these instances, the optimal combination (which

includes a moisture variable) leads to more realistic trends, thus confirming the role that the drying in the South-East of Australia has had on some temperature trends.

- Overall, the ability of the technique to reproduce non-stationarities in the climate record (a fully cross-validated test) is only slightly less than the ability to reproduce observed trends.

- The increase of frost occurrences has been documented; it is limited to the central and eastern parts of inland SEA at low elevation and to the start and end of the frost seasons. Although the optimised SDMs are capable of reproducing some aspects of the long-term trends for frost occurrences, it is proving more challenging than mean T_{min}, suggesting the importance of much localised effects not captured by the downscaling technique. The observed frost increases are due to a combination of synoptic trends (particularly important in autumn) and moisture changes.

Technical details

Update on methodology and preliminary comments

The original project scope was broadened and more analyses were performed. To complete these additional tasks, the project was extended for 6 months and the final report has been delayed accordingly.

- Following on the evaluation of the performance of the individual Statistical Downscaling Models (SDMs) (Timbal et al., 2008) in 3 SEACI sub-domains, project 1.4.1 objectives were to go one step further and analyse the ability of the SDMs to capture observed long-term trends. This validation is important to ensure that the large-scale predictors are capturing the forcing that explains local trends. It is a pre-requisite step before applying the technique to simulations of the 20th century to investigate the possible attribution of observed trends to external forcings (project 1.5.1).

- Linear trends were fitted to observed data and compared with similar trends from reconstructed series based on the optimised SDMs applied to the entire length of the available record (from 1958 to 2006) whenever possible. However, due to data limitations, trends for pan-evaporation are calculated from 1975 to 2003 and from 1958 to 2003 for dew point temperature. As discussed earlier (Timbal et al., 2008 and project 1.4.1 six-monthy reports), the technique underestimates day to day variability with a flow-on effect on the ability to reproduce inter-annual variability which, in turn, affects linear trends. This shortcoming is dealt with by using “normalised” trends: linear trends calculated at any locations for the analogue reconstructed series are divided by the percentage of the inter-annual variability observed at the local station captured by the SDMs. In this report, normalised trends are discussed unless otherwise stated.

- The focus of this project has been the observed rainfall decline. Results have been restricted to two of the three regions for which the Bureau Statistical Downscaling Model (SDM) was optimised for during project 1.3.1: the South-West of Eastern Australia (SWEA) and the Southern Murray-Darling (SMD). The third region (the South Eastern Coast, SEC) was not used principally because of earlier results showing that on-going trends, in particular for rainfall, are different between the eastern coastal eastern Australia and the inland areas (Timbal et al., 2007; Rakich et al., 2008). SMD and SWEA cover most of the SEACI region (apart from Eastern Gippsland) and encompass in full the

area of significant rainfall decline across South Eastern Australia (SEA) (Murphy and Timbal, 2007).

- The purpose of a SDM is to provide local information and, hence, the usefulness of such a method greatly depends on the spatial coverage of available observations. The level of details contained in the report reflects this and depends on the number of stations available for each variable: 324 rainfall stations were used and the ability of the technique to reproduce local rainfall trends is reported in greater details; 41 temperature stations were used, which warrants the evaluation of spatial structures; for pan evaporation (14 stations) and dew-point temperature (five stations) only regional averages are discussed.

- Beyond the ability of the technique to reproduce observed trends, a further validation was done by splitting the record into earlier (wetter and cooler) and latter (dryer and warmer) periods. This fully cross-validated test, although not essential to apply the technique to simulation of the 20th Century, is critical before using the technique for future projections. It responds to the concern that SDM relies on the stationarity of the statistical linkage between predictors and predictands, which is often cited as a possible short-coming in providing downscaled future projections using SDMs. Although not part of the original project proposal, it was though to be a useful complement, providing insight into the ability of the technique to describe on-going shifts in the climate record and ensuring that future projections based on the BoM SDM (as proposed as part of a future extension of SEACI) will be based on solid evidence of the applicability of the technique.

- The SDM produces daily values and hence the full probability distribution functions (PDFs) can be calculated. This is an opportunity to focus on extreme values. Recently, the occurrence of frost in SEA has become topical due to recent cases of late and damaging frosts. This perceived increase in frost occurrences is somewhat contradictory to the on-going global warming. Although not part of the original project, it was decided to take advantage of the calculations already performed and analyse our results further to evaluate the ability of the technique to reproduce local frost occurrences and investigate these observed frost trends.

Reproduction of the drying trends across SEA

The ability of the technique to reproduce observed rainfall is first assessed from a regional perspective looking at seasonal averages across all stations (Table 1) in the two climate entities: the South-West of Eastern Australia (SWEA) and the Southern Murray Darling Basin (SMD). The largest signal, the autumn rainfall decline, is well reproduced (80 per cent in SWEA and 60 per cent in SMD using normalised trends and 100 per cent in SWEA and 75 per cent in SMD without normalisation). It is worth noting that the normalisation of the trends does not improve the results. This indicates that the inflation factor used for rainfall to reduce the underestimation of variance (Timbal et al., 2008; 2009a) is effective and there is no additional gain in normalising trends.

Regional features are captured: negative (vs. positive) trends in summer and spring in SMD (vs. SWEA), while local trends are reproduced with some skill (spatial correlation between linear trends calculated on the observed and reconstructed series, after normalisation, varies between 0.25 and 0.57). These correlations are significant (at the 95 per cent level) but not very high, as visible from the scatter diagrams (Fig. 1) showing observed vs analogue linear trends at the 324 SEACI stations. The slope of the best fit line is high in summer (0.70) and autumn (0.62) (a value of 1 would be a perfect match), but low in winter (0.45) and spring (0.26) when most analogue

reconstructed series show modest positive rainfall trends between 0 and 1 mm.day^{-1}/century while the trends in the observations vary greatly between -1.5 and 1.5.

The analysis of SDMs using a single predictor (Fig. 2) shows that in most instances (seven out of eight cases) MSLP alone produces linear trends which encompass the observed trends (based on six SDMs sampling the uncertainties of the statistical linkage). The mean of the six SDMs usually provides a trend of the right sign and of a magnitude comparable to the observations. Linear trends produced by the optimised SDMs are not a simple addition of the linear trends produced by individual predictors due to existing relationships between large-scale atmospheric variables. But providing that the large-scale forcings are complementary (such as a combination of synoptic, moisture and thermal variables), then the optimised model will combine the influence of each individual predictor. In this light, it is worth noting that moisture variables (principally Q_{850}) exhibit small linear trends of the right sign which, combined with the MSLP influence, are likely to provide a better match to the observations: e.g. the negative trends in autumn are likely to enhance the negative trends produced with MSLP, and the small positive trends in summer are likely to reduce the negative trend produced by the synoptic (captured by MSLP) changes. In some instances, wind components are used in the optimal combination of predictors (predictors used in optimised SDMs are highlighted by red boxes in Fig. 2) and generate trends which are likely to provide a better match to the observations.

The ability to reproduce observed trends is part of the statistics used to evaluate and optimise the SDM. It is worth emphasis, that it is not the most important aspect evaluated: the optimised combination of predictors relies mostly on analysis of the day-to-day skill and the ability to reproduce the main moment of the series (Timbal et al, 2008; 2009a). The choice of optimised combinations of predictors was not influenced by this analysis: i.e. the best combination of predictors was not chosen to ensure the best possible reproduction of the observed trends. This is an independent test which only purpose it shed light on the large-scale changes which help explain on-going trends.

Reproduction of the warming trends

The ability of the SDM to reproduce observed warming is first assessed from a regional perspective looking at seasonal averages across all stations in the two climate entities (SWEA and SMD) for T_{max} (Table 2) and T_{min} (Table 3). Contrary to rainfall, the underestimation of warming trends due to the underestimation of the variance (there is no correction factor for temperature) is very clear. The normalisation (right columns) of the trends (factoring in the underestimation of the inter-annual variability) eliminates the systematic biases, as differences between trends from the observations and the reconstructed series are either positive (six cases) or negative (10 cases) across the two predictands, two regions and four seasons. Some warming trends are still largely underestimated: T_{max} in summer in both regions and in autumn in SWEA for both T_{max} and T_{min}. In contrast, the analogue reconstructed series are warming too strongly in spring for T_{max} in both regions and in winter and spring for T_{min} in SMD.

The ability of the technique to capture local features of the temperature trends is assessed by the correlations between linear trends for observed and analogue reconstructed local series (41 in total). Correlations are in most instances significant (at the 95 per cent level shown as bold figures in Table 2 and 3) but low: from 0.20 for T_{max} in autumn to 0.61 for T_{min} in autumn. Across all the stations and all the seasons the slope of the best fit between the observed and reconstructed series linear warming is reasonable: 0.75 for T_{max} (Fig. 3) but only 0.49 for T_{min} (Fig. 4). However, season by season (as can be seen from the colour code), the scatter of points is relatively “flat” suggesting that very little of the station to station differences in warming trends is being captured. This is particularly true for T_{max} as measured by the spatial correlations in Table 2.

The analysis of SDMs using a single predictor shows that, in most instances, tropospheric warming (T_{850}) provides the largest warming trends of any single predictor and, in 6 instances (Fig. 5 and 6), matches the observed trends. In contrast, MSLP, as a predictor, hardly suggests any warming trends and in some cases (mostly in autumn for both region and both T_{max} and T_{min}) points toward large cooling trends. Additional predictors such as Q_{850} for T_{min} are also likely to contribute to the trends from the analogue model using the optimal combination of predictors.

Reproduction of trends for the additional variables

The ability of the SDM to reproduce observed trends for additional variables relevant to the hydrological surface balance has only been assessed from a regional perspective, looking at seasonal averages across all stations in the two climate entities (SWEA and SMD) for pan-evaporation (Table 4) and dew-point maximum (DT_{max}, Table 5) and minimum (DT_{min}, Table 6) temperatures.

As was the case for temperature, the underestimation of observed trends is very large and strongly relates to the underestimation of the variance (there is no correction factor for these variables). The normalisation of the trends (factoring in the underestimation of the inter-annual variability) eliminates the systematic biases and results in trends either larger or smaller than observed.

In all cases except for pan-evaporation in winter in SMD, the sign of the predictand trends is captured by the technique. The magnitude in most instances is within +/- 30 per cent of the observed values but with some notable exceptions: pan-evaporation in autumn in SMD and in spring in SWEA, DT_{min} in autumn and spring in both regions and DT_{max} in winter in SMD.

Reproduction of the non-stationarities in the climate record:

In this evaluation, the analogue models are optimised on the 1958–1990 calibration period and then applied to the 1991–2006 period, with the analogue selected from the calibration period, thus ensuring a full cross-validation and an evaluation of the ability of the technique to reproduce a shift in the climate. The magnitude of the changes between the latter part of the climate observational record in SEA and the earlier part makes this exercise meaningful when considering the application of SDMs for future climate change projections (Table 7). This is particularly true for rainfall, where the magnitude of the rainfall decline in autumn (-30 per cent across the 324 stations in SWEA and SMD) is as large as any future projections. In contrast, temperature changes (mostly warming apart for T_{min} in autumn) range between 0.15 °C and 0.54 °C and are an order of magnitude smaller than future projections by 2050. Based on results from the reproduction of the trends, results for rainfall are not "normalised" but they are normalised for temperature (i.e. the ΔT calculated from the analogue series is divided by the amount of inter-annual variability reproduced in the 1991–2006 period).

Overall, the results for this cross-validated exercise should be analysed and compared to the results discussed earlier regarding the ability of the SDMs to reproduce the observed trends over the entire period (not cross-validated). In general, the ability of the SDM to reproduce the observed changes (spatial correlation in Table 7, slope of the best fit in Fig. 7 and Fig. 8) resemble those obtained earlier and only show a slight reduction in the overall performance of the SDM. Noteworthy, is the SDM reproduction of the dryer recent period: the rainfall reduction in autumn is underestimated (70 per cent of the observed change is reproduced, which is comparable to the ability of the SDM to reproduce the trends); however, a decline in winter and spring is produced by the analogue reconstruction which is not apparent in the observed series. The reproduction of

the observed ΔT is satisfactory apart for T_{max} in autumn and T_{min} in spring where the sign is wrong, albeit for very small values. The slope of the best fits (Fig. 8) is similar for T_{min} (0.55 compared to 0.49 for the trends: Fig. 8b vs. Fig. 4) but reduces for T_{max} (0.41 instead of 0.75: Fig. 8a vs. Fig. 3).

Using the Bureau of Meteorology SDM to understand trends in frost occurrences:

This climatological analysis was performed on a subset of the 56 stations identified in SEA. Stations with missing years after 1958 and coastal stations with very few frost occurrences (FO) were removed. In total, 23 stations were used. 905 FO are observed across that network per year (Fig. 9), with two thirds occurring during the winter months (JJA). The inter-annual variability is large (STD = 184) and linked to the El Niño Southern Oscillation (ENSO). The correlation with the SOI is -0.38 (-0.36 in JJA). Peaks of FO during El Niño years are clearly visible along the historical record (red circles in Fig. 9). This is consistent with the known impact of ENSO on SEA climate: lower rainfall, higher maximum temperature and lower minimum temperature and hence higher FO (Murphy and Timbal, 2007). The physical mechanism is the higher number of high pressure systems developing above SEA favouring dry conditions, clear skies and cool nights. This is best diagnosed by looking at the relationship between the Sub-Tropical Ridge intensity (STR-I) as diagnosed by Drosdowsky (2005). The STR over SEA reaches its northern-most location in winter (30 °S) and shifts south in spring (31 °S) and autumn (34 °S). The relationship between STR-I and FO is stronger than the relationship between the SOI and FO: r=0.41 all year around and r=0.59 in JJA (both significant at the 99 per cent level). In autumn the relationship is weak (r=0.37); it is insignificant in spring (r=0.09).

The long-term trend is small and insignificant: +31 occurrences over 50 years across all stations limited to the shoulder seasons: +12 in autumn and +25 in spring and a very small decline in winter. These small spatial averages hide important geographical features: there are a near equal number of stations with positive (7) or negative (8) large (and statistically significant at the 95 per cent level) trends. Stations with decreasing FO tend to be located in Western Victoria and South Australia (Mount Baker, Mount Gambier, Lameroo, Ouyen and Mildura), while stations with large positive trends are located further east (Horsham, Ballarat, Echuca, Rutherglen, Sale and Orbost). Stations at higher elevations in the Great Dividing Range (Omeo, Canberra) are experiencing reduced FO.

Overall the SMD reproduces the total number of FO across SEA exactly (905 cases per year), the inter-annual variability is well captured (r=0.82) but underestimated (STD=117 versus 184 observed). The long-term trend is as small and insignificant as observed but with the opposite sign (Fig. 9). Details on the seasonality of the trends (positive in the shoulder seasons, negative in winter) are well captured by the analogue reconstruction (Table 8, right columns) but with a bias toward more negative trends. Analysis of the month-by-month trends (Fig. 10) confirms this: the largest error is for the month of August where a strong increase in FO is hardly captured by the analogue reconstruction.

The large-scale forcing of the FO trends was investigated by comparing the analogue reconstructed series with SDMs using: 1) only MSLP, 2) MSLP combined with T_{850} and 3) the optimised SDMs where a moisture variable is always added and sometimes a wind field. MSLP is a critical predictor in capturing the FO trends (Table 8). It is interesting that, while MSLP has limited value in capturing temperature trends overall, it is important for T_{min} and, in particular, in getting the negative trends in autumn. In particular, it generates a larger than observed negative trends for T_{min} and a larger than observed positive trend for FO; this is consistent with earlier results (shown in the second row of Fig. 6). And as shown here, it is very important for the lower tail of the distribution (i.e. frost occurrences). Once the thermal predictor is added, the surface warming is stronger than observed, and also the FO reduction. Finally, with an additional

moisture variable added, trends get closer to the observed values for both T_{min} and FO. Besides the importance of using a combination of predictors to best capture the observed trends (arguably MSLP alone performed better than the optimised SDM), the added skill for the more complex SDM is shown by looking at its ability to reproduce local trends as measured by the correlation between observations and the analogue reconstructed series for the 23 locations (Table 9). Correlations are always higher with the optimised model (very much so when compared to the SDM using MSLP only) and, apart for FO in autumn, is always statistically significant at the 95 per cent level.

Overall, local trends in FO and minimum temperature are a combination of the on-going global warming (captured by T_{850}), limited by circulation changes (captured by MSLP) leading to a surface cooling in autumn and an increase in FO and complemented by associated moisture changes (drying in autumn which reinforced the FO increase, not so in winter). Based on the evidences presented here, it is hard to claim that circulation changes explain the local trends for T_{min} during the autumn-winter-spring part of the year since the seasonality and magnitude of the trends appears to be more complex and involve global temperature increases and local moisture changes. This is reminiscent of earlier findings that circulation changes could not explain the recent extreme heat wave of April 2005 (Timbal et al., 2007).

Conclusions

This project completes the evaluation of the BoM SDM for six surface predictands across the entire SEACI region. Besides the technique's ability to reproduce local PDFs and skilfully capture day-to-day and inter-annual variability (project 1.3.1), the technique was found capable of reproducing many features of the observed climatic trends across the regions. It appears to be a suitable tool to apply to simulation of the 20th Century climate and is likely to improve on the use of climate model direct outputs in the quest to attribute these observed changes to known external forcings (project 1.5.1). In addition, a better understanding of which large-scale changes are responsible for the observed local changes has been gained and documented. Finally, the BoM SDM appears able to reproduce the local observed climate shift. This finding, combined with the availability of downscaled climate change projections Australia-wide for six different predictands based on the latest crop of IPCC-AR4 models (Timbal et al., 2009b), makes it a very suitable tool to generate local climate change projections across the SEACI domain.

Additional information

Acknowledgement:

This work was funded by the South Eastern Australia Climate Initiative.

References:

Drosdowsky, W., 2005: The latitude of the subtropical ridge over eastern Australia: the L index revisited. *International Journal of Climatology*, **25**, 1291-1299

Murphy, B.F. and B. Timbal, 2007: A review of recent climate variability and climate change in south eastern Australia. *International Journal of Climatology,* **28(7)**, 859-879

Rakich, C., N. Holbrook and B. Timbal, 2008: A pressure gradient metric capturing planetary-scale influences on eastern Australian rainfall. *Geophysical Research Letters,* **35**, L08713, doi:10.1029/2007GL03297

Timbal B. and B. Murphy. 2007: "Document changes in south-eastern Australian rainfall, temperature, surface humidity and pan evaporation". South-Eastern Australian Climate Initiative (SEACI), final report for project **1.1.1**, 19 pp

Timbal, B., B. Murphy, K. Braganza, H. Hendon, M. Wheeler and C. Rakich. 2007: "Compare documented climate changes with those attributable to specific causes". South-Eastern Australian Climate Initiative (SEACI), final report for project **1.1.2**, 19 pp

Timbal**,** B., B. Murphy, E. Fernandez and Z. Li. 2008: "Development of the analogue downscaling technique for rainfall, temperature, surface humidity and pan evaporation". South-Eastern Australian Climate Initiative (SEACI), final report for project **1.3.1**, 17 pp

Timbal, B., E. Fernandez and Z. Li, 2009a: Generalization of a statistical downscaling model to provide local climate change projections for Australia. *Env. Mod. & Software,* **24**, 341-358

Timbal, B., Z. Li and E. Fernandez, 2009b: "The Bureau of meteorology Statistical Downscaling Model Graphical User Interface: user manual and software documentation", *CAWCR research report*, **4**, pp 95 (http://www.cawcr.gov.au/publications.php)

Outputs from this project

Timbal, B., E. Fernandez and Z. Li, 2009: Generalization of a statistical downscaling model to provide local climate change projections for Australia. *Env. Mod. & Software,* **24**, 341-358

Timbal, B., Z. Li and E. Fernandez, 2009: "The Bureau of meteorology Statistical Downscaling Model Graphical User Interface: user manual and software documentation", *CAWCR research report*, **4**, pp 95 (http://www.cawcr.gov.au/publications.php)

Appendix: figures and tables

Table 1: *Summary statistics for each calendar seasons of the rainfall linear trends computed from 1958 to 2006 and averaged across all stations in two regions (SMD and SWEA): observed (left two columns), reproduced by the analogue models (columns 3 and 4) and then normalised by the amount of interannual variability reproduced by the analogue model (columns 6 and 7). The spatial correlations across the 324 stations (SMD and SWEA combined) are shown in columns 5 and 8 (bold values are statistically significant at the 95 per cent level). Trends are in mm.day^{-1} per century.*

mm/day^{-1} per century	Observation		Analogue			Analogue normalised		
	SMD	SWEA	SMD	SWEA	r	SMD	SWEA	r
Summer	-0.30	0.13	-0.55	0.60	**0.55**	-0.42	0.58	**0.57**
Autumn	-1.13	-1.06	-0.80	-1.03	**0.17**	-0.69	-0.85	**0.37**
Winter	0.33	0.28	0.38	0.43	**0.37**	0.33	0.63	**0.40**
Spring	-0.20	0.02	-0.18	0.25	**0.21**	-0.22	0.36	**0.25**

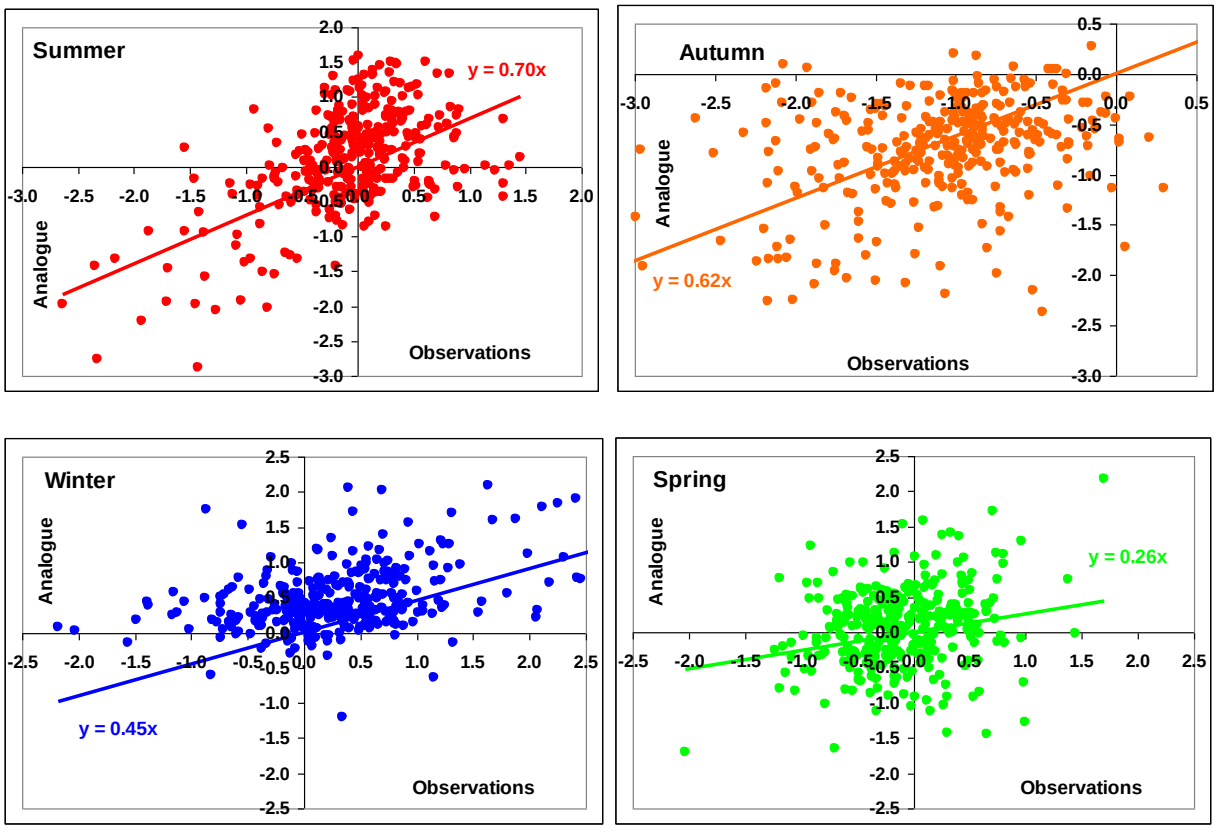

Fig 1: *Reproduction of the observed rainfall trends (in mm.day^{-1} per century) using 324 rainfall stations across the SEACI regions SMD and SWEA (a season per plot). Each point has for the x-coordinate the observed linear trends computed between 1958 and 2006 and the normalised trend for the analogue reconstructed series as y-coordinate. Linear best fits are fitted through the origin (0, 0) and their slopes are shown on each graph.*

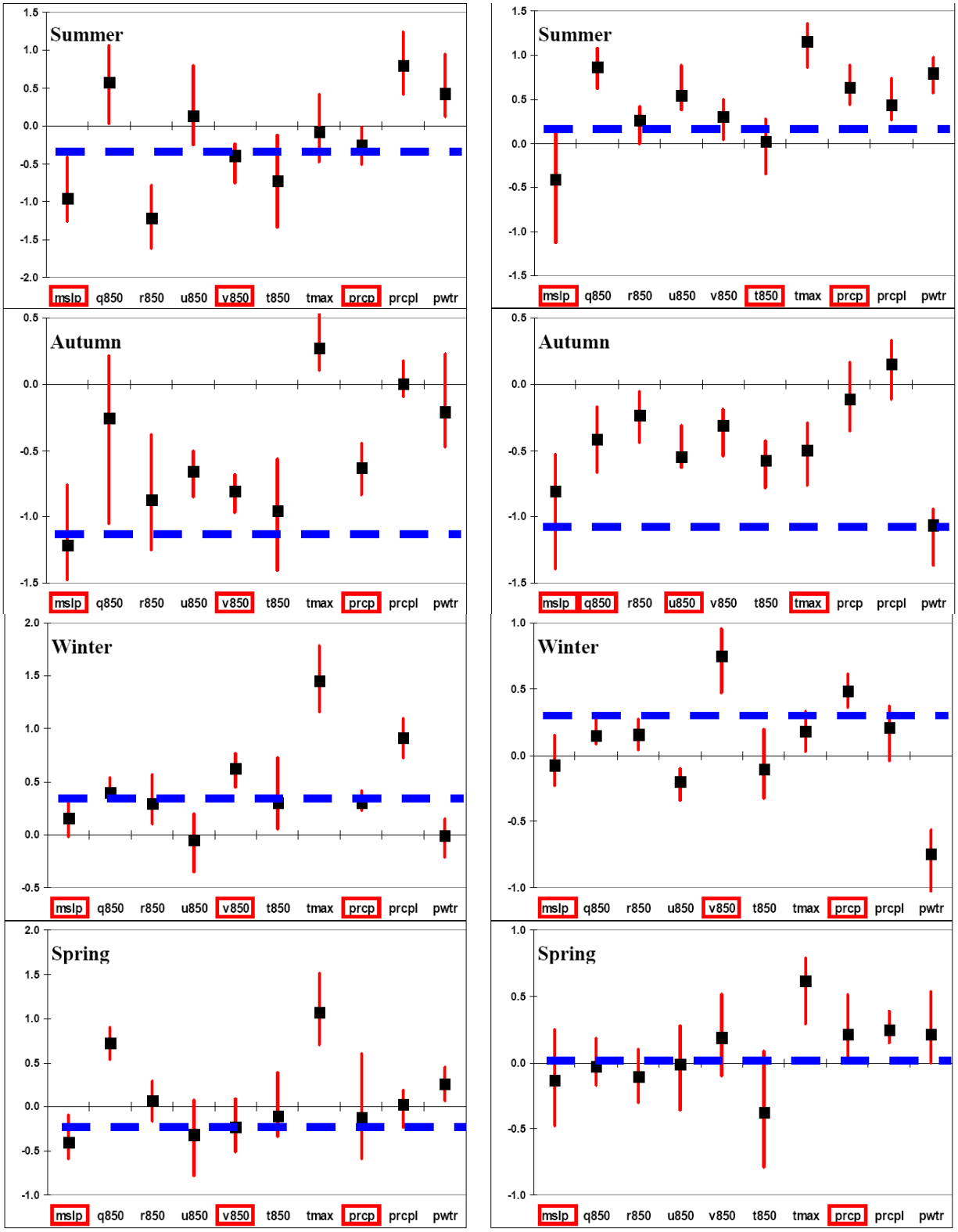

Fig 2: *1958 to 2006 Linear trends averaged across all rainfall stations in SMD (left) and SWEA (right) for the four seasons (summer to spring from top to bottom) fitted on analogue reconstructed series based on a single predictor (predictors included in the optimal combinations are indicated by red squares. Black squares show the mean of six SDMs, while the red bars show the full range; magnitudes of the observed trends are indicated by dashed blue lines.*

Table 2: *Summary statistics of the reproduction of the observed trends for T_{max} as per Table 1. Units are in °C per century.*

°C per century	**Observation**		**Analogue**			**Analogue normalised**		
	SMD	SWEA	SMD	SWEA	r	SMD	SWEA	r
Summer	2.16	1.51	0.57	0.77	**0.45**	1.07	1.16	**0.48**
Autumn	1.65	1.48	0.76	0.07	0.21	1.42	0.08	0.20
Winter	1.57	1.58	1.12	0.72	0.23	2.30	1.34	0.29
Spring	1.81	1.73	1.24	1.49	**0.39**	2.86	2.35	**0.47**

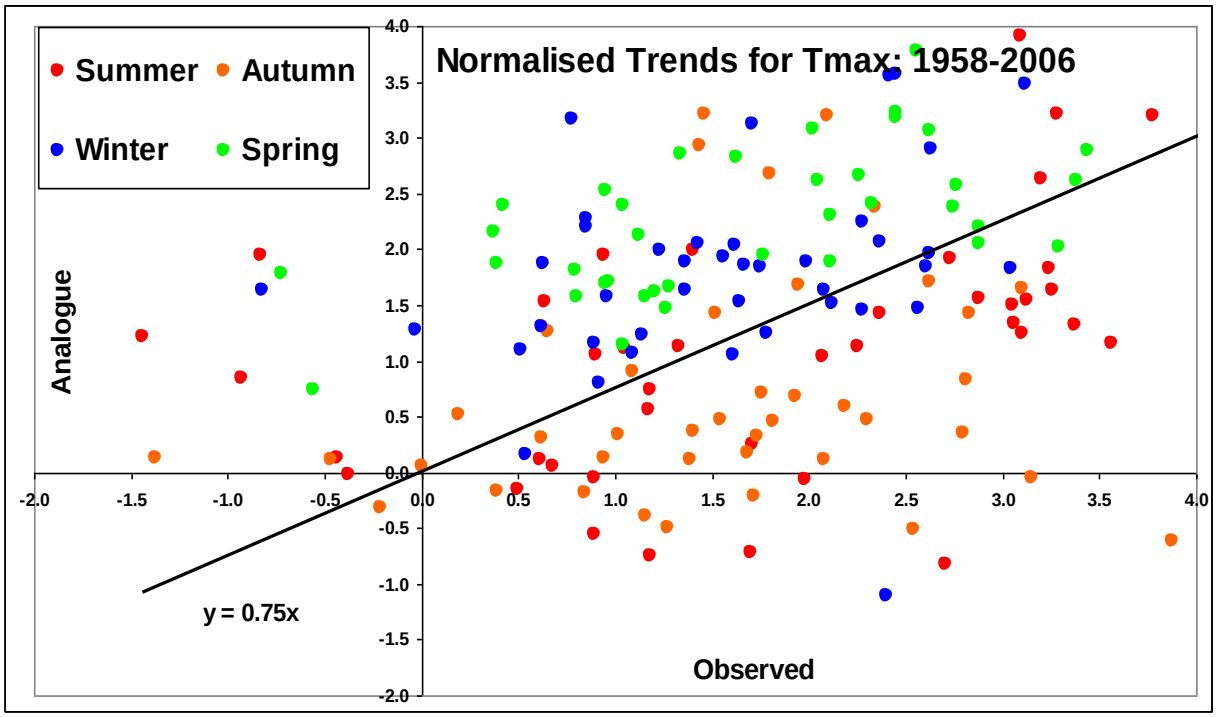

Fig 3: *Reproduction of the observed trends for T_{max} for the 41 temperature stations across the SEACI regions (SMD and SWEA combined); the four calendar seasons are shown on a single graph using colour code. Each point has for the x-coordinate the observed linear trends computed between 1958 and 2006 and the normalised trend for the analogue reconstructed series as y-coordinate. Linear best fits fitted through the origin (0, 0) across all data points (4 seasons together) and their slopes are shown on the graph.*

Table 3: *As per Table 2 but for T_{min}.*

°C per century	Observations		Analogues			Analogue normalised		
	SMD	SWEA	SMD	SWEA	r	SMD	SWEA	r
Summer	1.27	1.20	0.69	0.60	**0.49**	1.19	1.15	**0.57**
Autumn	-0.61	0.06	-0.36	-0.55	**0.47**	-0.73	-0.99	**0.61**
Winter	0.32	1.44	0.90	0.56	**0.35**	1.90	1.45	0.30
Spring	0.46	1.20	0.90	0.55	0.29	1.59	1.02	**0.36**

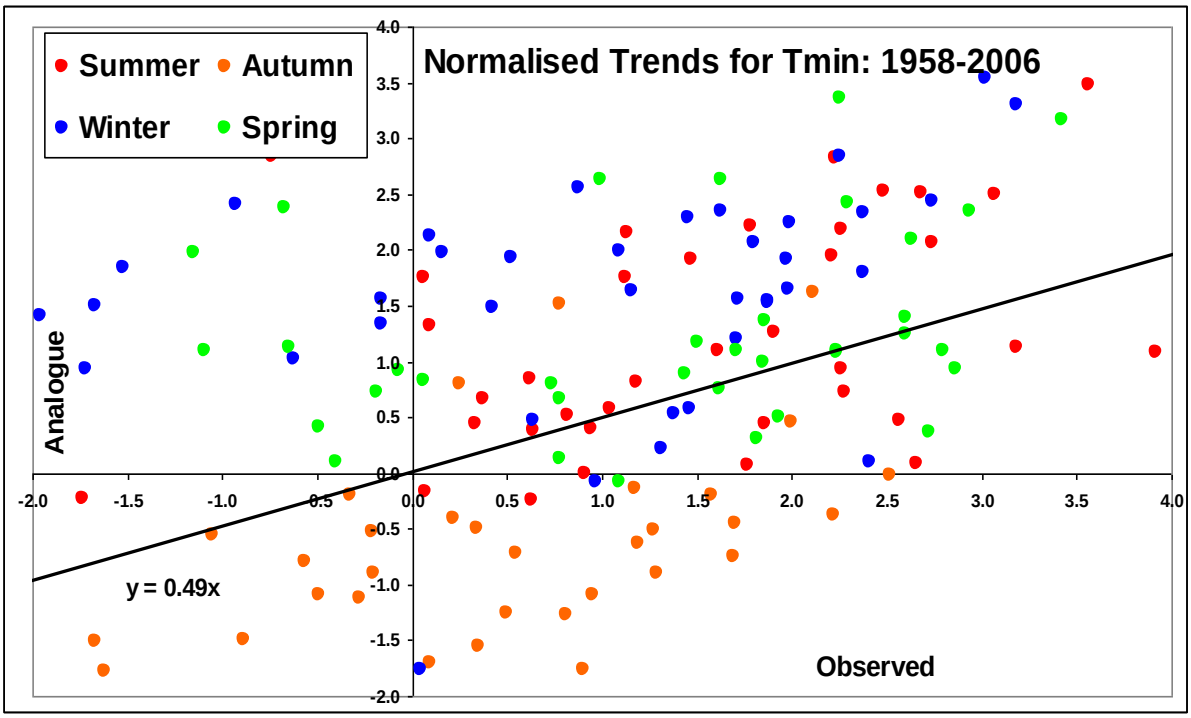

Fig 4: *As per Fig.3 but for T_{min}.*

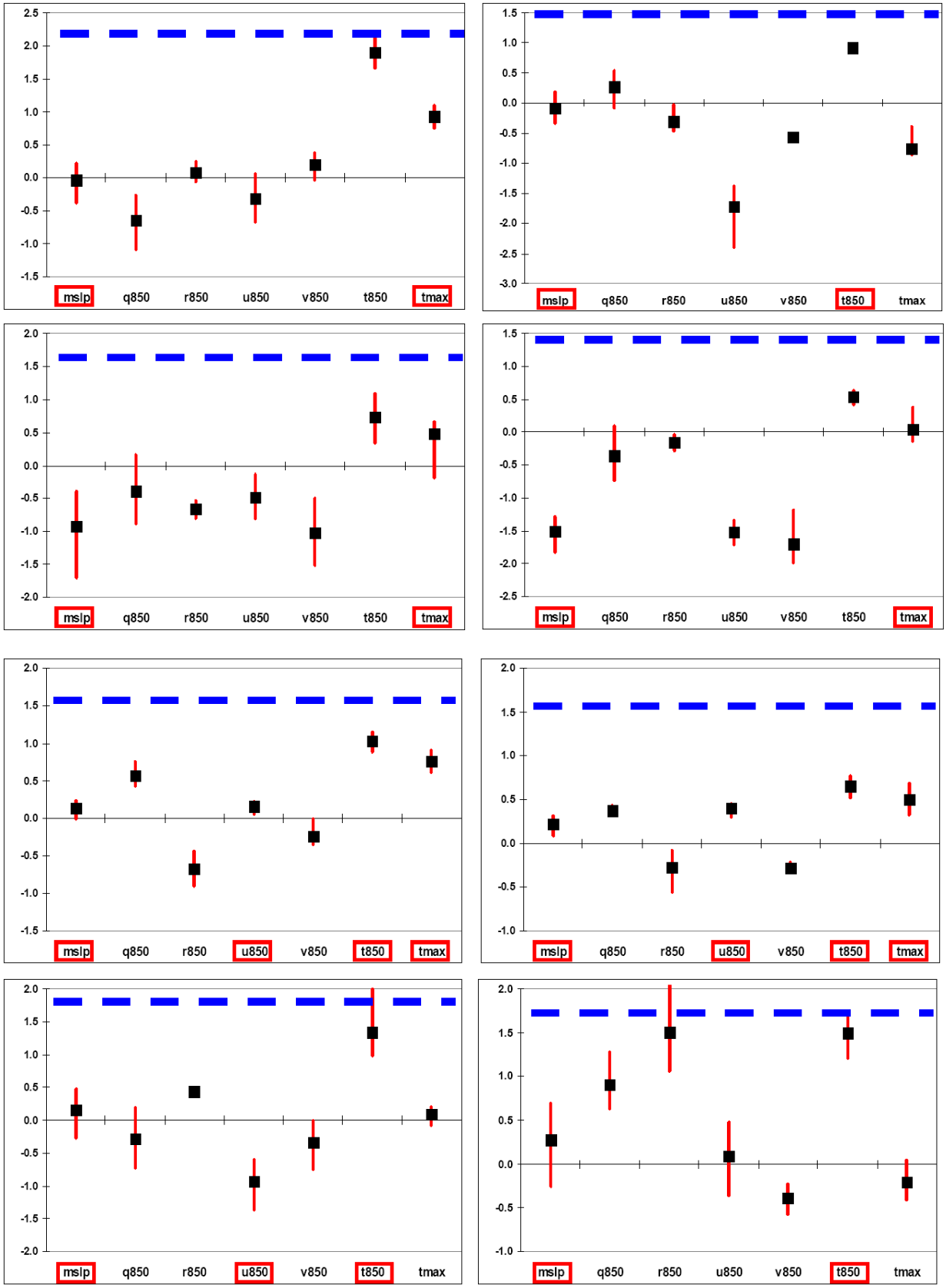

Fig 5: *As per Fig. 2 but for T_{max} (left column for SMD and right column for SWEA, summer to spring from top to bottom).*

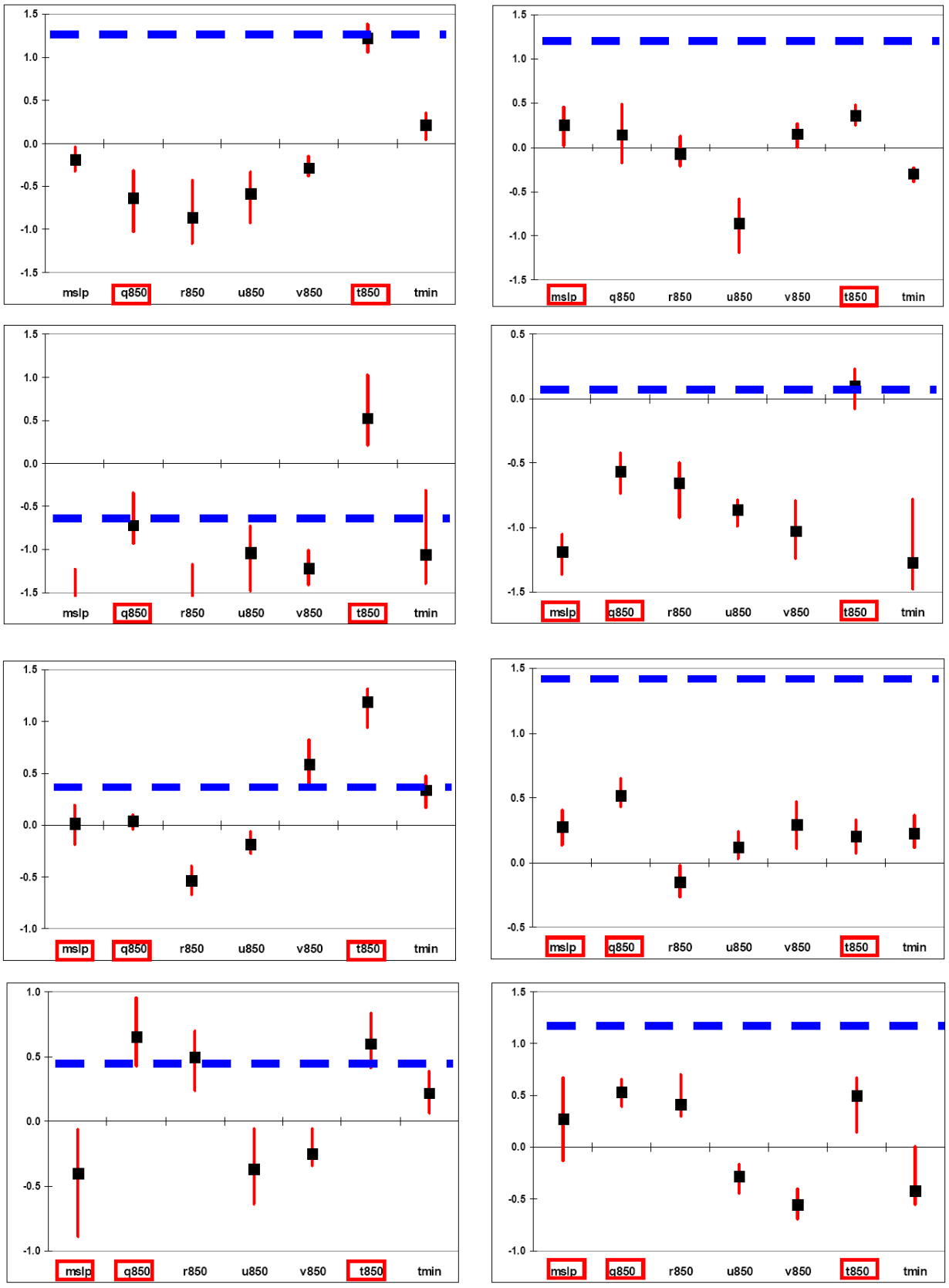

Fig 6: *As per Fig. 2 but for T_{min} (left column for SMD and right column for SWEA, summer to spring from top to bottom).*

Table 4: *Summary statistics of the reproduction of the observed trends from 1975 to 2003 for pan-Evaporation as per Table 1 (units are in mm.day^{-1} per century)*

mm.day^{-1} per century	**Observation**		**Analogue**		**Analogue normalised**	
	SMD	SWEA	SMD	SWEA	SMD	SWEA
Summer	-3.48	-1.56	-1.41	-0.64	-4.73	-1.69
Autumn	-1.60	-0.98	-0.08	-0.55	-0.20	-1.29
Winter	-0.57	-0.14	0.19	0.00	0.40	0.00
Spring	-1.17	-1.16	-0.35	-0.61	-1.35	-1.67

Table 5: *Summary statistics of the reproduction of the observed trends from 1958 to 2003 for dew-point maximum temperature as per Table 1 (units are in °C per century)*

°C per century	**Observation**		**Analogue**		**Analogue normalised**	
	SMD	SWEA	SMD	SWEA	SMD	SWEA
Summer	-1.17	1.18	-0.68	0.42	-1.17	0.97
Autumn	-0.92	1.46	-0.59	0.49	-1.25	1.04
Winter	0.88	1.52	0.07	0.42	0.24	0.88
Spring	0.38	1.14	0.55	0.30	1.51	0.60

Table 6: *Summary statistics of the reproduction of the observed trends from 1958 to 2003 for dew-point minimum temperature as per Table 1 (units are in °C per century).*

°C per century	**Observation**		**Analogue**		**Analogue normalised**	
	SMD	SWEA	SMD	SWEA	SMD	SWEA
Summer	-6.67	-0.12	-0.92	-0.05	-2.99	-0.10
Autumn	-2.14	0.77	-0.40	-0.04	-0.84	-0.07
Winter	0.81	0.76	0.21	0.23	0.86	0.44
Spring	-3.07	-0.54	-0.08	-0.06	-0.39	-0.15

Table 7: *Summary statistics for three surface predictands (T_{max}, T_{min} and Rainfall) of the ability of the technique to reproduce the observed changes between 1991-2006 and 1958-1990. Values are averages across all available stations in SWEA and SMD combined (41 for temperature and 324 for rainfall, in °C for temperature and percentage for rainfall) and calculated for the observations (ΔO) and for the fully cross validated analogue reconstructed values for 1991-2006 (ΔA_{XV}). Spatial correlations between the observed and analogue reconstructed Δ at each station are indicated in a third column (correlation in bold are significant at the 95 per cent level). Analogue reconstructed temperatures are "normalised" but rainfall is not.*

	Summer			**Autumn**			**Winter**			**Spring**		
	ΔO	ΔA_{xv}	r	ΔO	ΔA_{xv}	r	ΔO	ΔA_{xv}	r	ΔO	ΔA_{xv}	r
T_{max}	0.40°	0.41°	0.27	0.27°	-0.16°	**0.34**	0.54°	0.48°	0.23	0.31°	0.68°	**0.35**
T_{min}	0.30°	0.24°	0.21	-0.48°	-0.60°	**0.55**	0.25°	0.01°	**0.31**	0.15°	-0.12°	0.18
Rain	11.6 per cent	7.3 per cent	-0.04	-30.7 per cent	-21 per cent	**0.55**	1.2 per cent	-10.6 per cent	**0.24**	5.1 per cent	-8.6 per cent	**0.21**

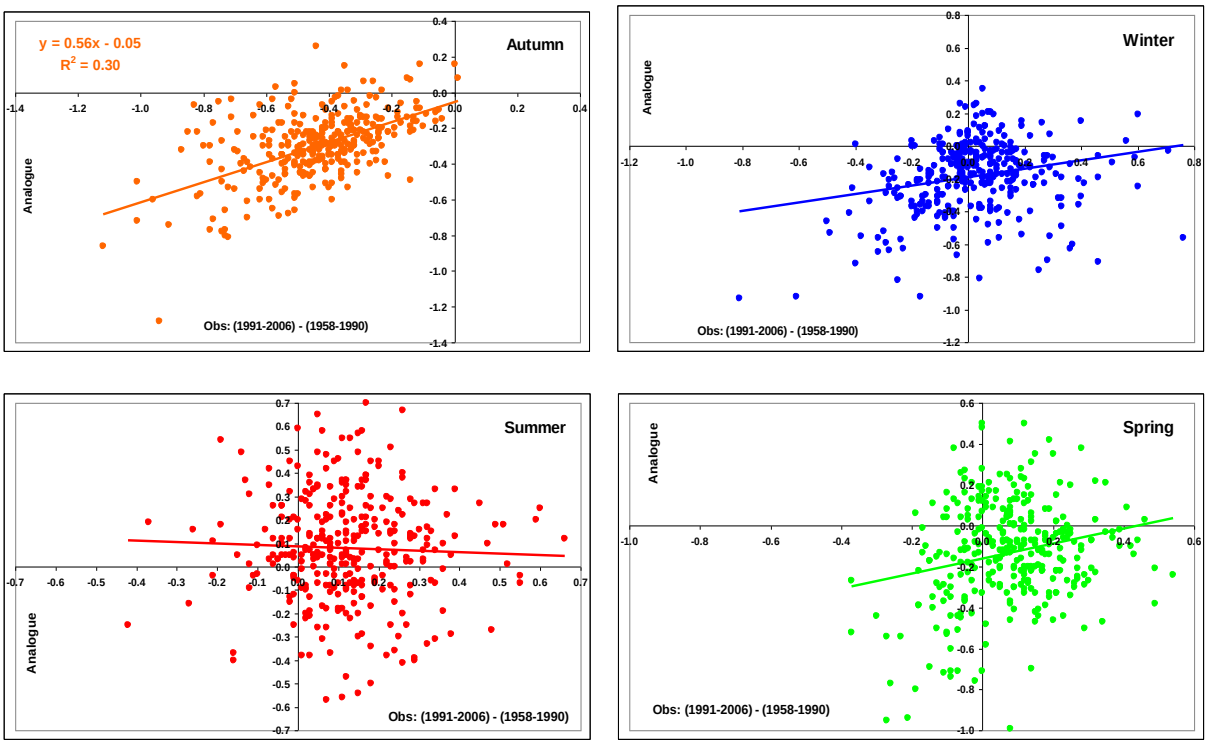

Fig 7: *Cross validated reproduction of the observed changes since 1990 for rainfall for the 324 rainfall stations across the SEACI regions (SMD and SWEA) and for the four calendar seasons. Each point has for x-coordinate the ΔR_{obs} (i.e. the 1991-2006 mean minus the 1958-1990 mean) from observations and the similar quantity from the analogue reconstructed as a y-coordinate. The 1991-2006 mean is fully cross-validated as it uses analogues from the 1958 to 1990 period. Linear best fits are shown on each graph.*

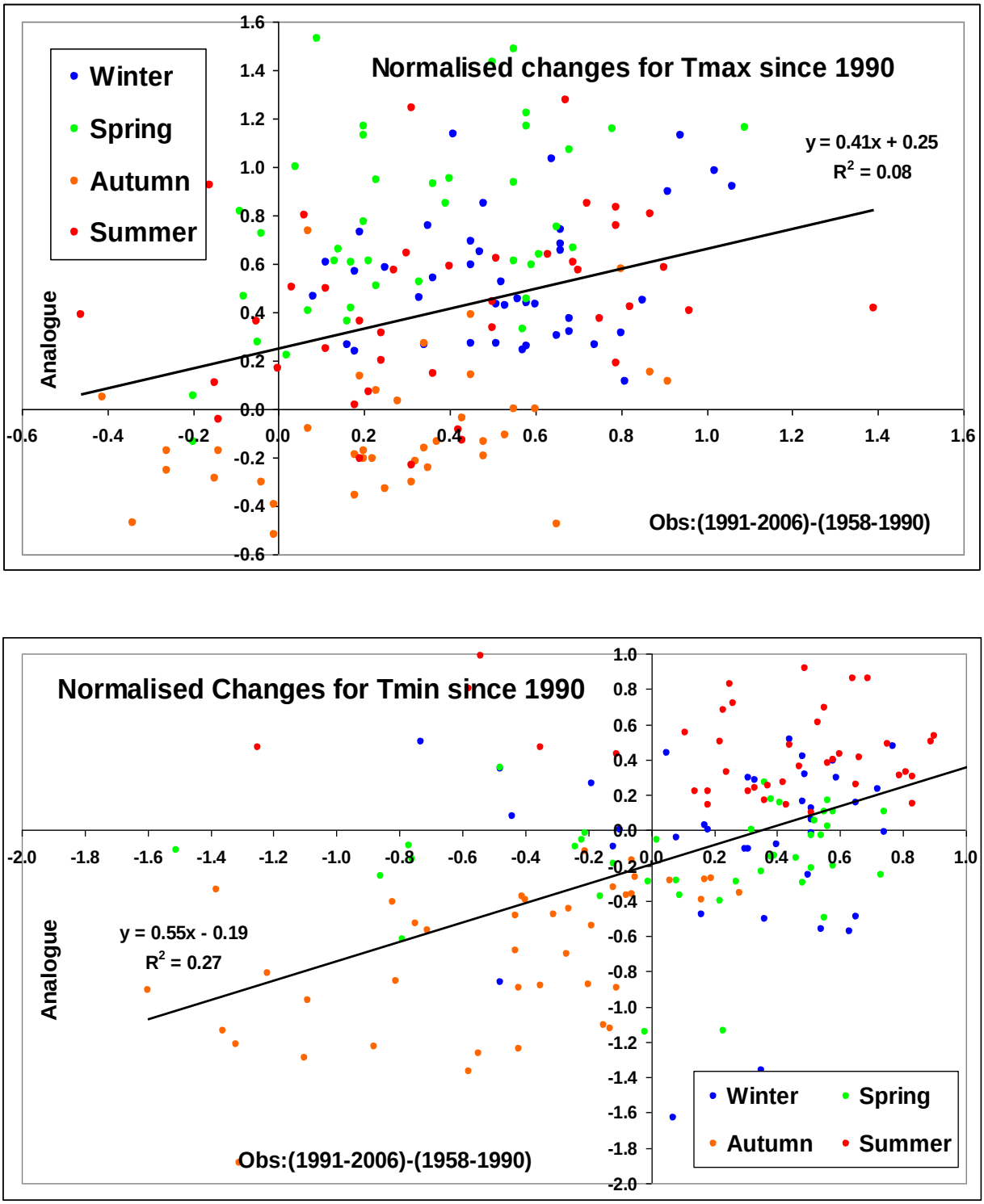

Fig 8: *As per Fig. 7 but for T_{max} (upper) and T_{min} (lower) for the 41 temperature stations across the SEACI region and for the four calendar seasons in one plot.*

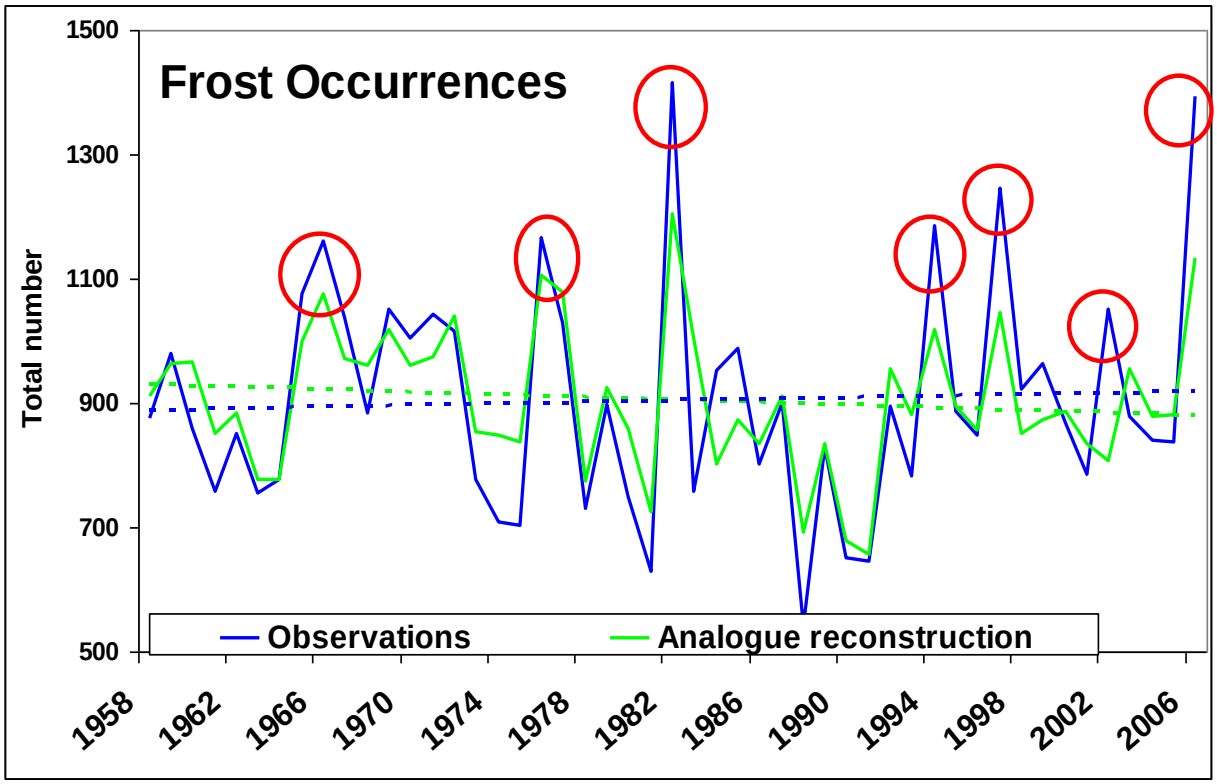

Fig 9: *Interannual variability of the total number of observed frost occurrences (minimum temperature below 2°C) all year around across 23 stations in SEA (blue lines) and for the analogue reconstructed series (green lines). Linear trends are shown as dashed lines. Major El Niño events during the period are indicated with red circles: 1965-66, 1977-78, 1982, 1994, 1997, 2002 and 2006.*

Table 8: *1958 to 2006 linear trends for frost occurrences (F.O in total number of days across SEA per 50 years) and T_{min} (in °C per century) in autumn, winter and spring from observations and analogue reconstructed series using as predictors: MSLP, MSLP combined with T_{850} and with the full optimised analogue model.*

	Observation		**MSLP only**		**MSLP & T_{850}**		**Optimised analogue**	
	F. O.	$<T_{min}>$	F. O.	$<T_{min}>$	F. O.	$<T_{min}>$	F. O.	$<T_{min}>$
Autumn	+12.0	-0.48	+21.2	-0.62	-5.7	+0.0	+3.6	-0.32
Winter	-6.7	+0.16	+11.5	+0.02	-43.5	+0.27	-55.5	+0.34
Spring	+25.1	-0.04	-0.5	-0.06	-21.5	+0.28	+4.3	+0.17

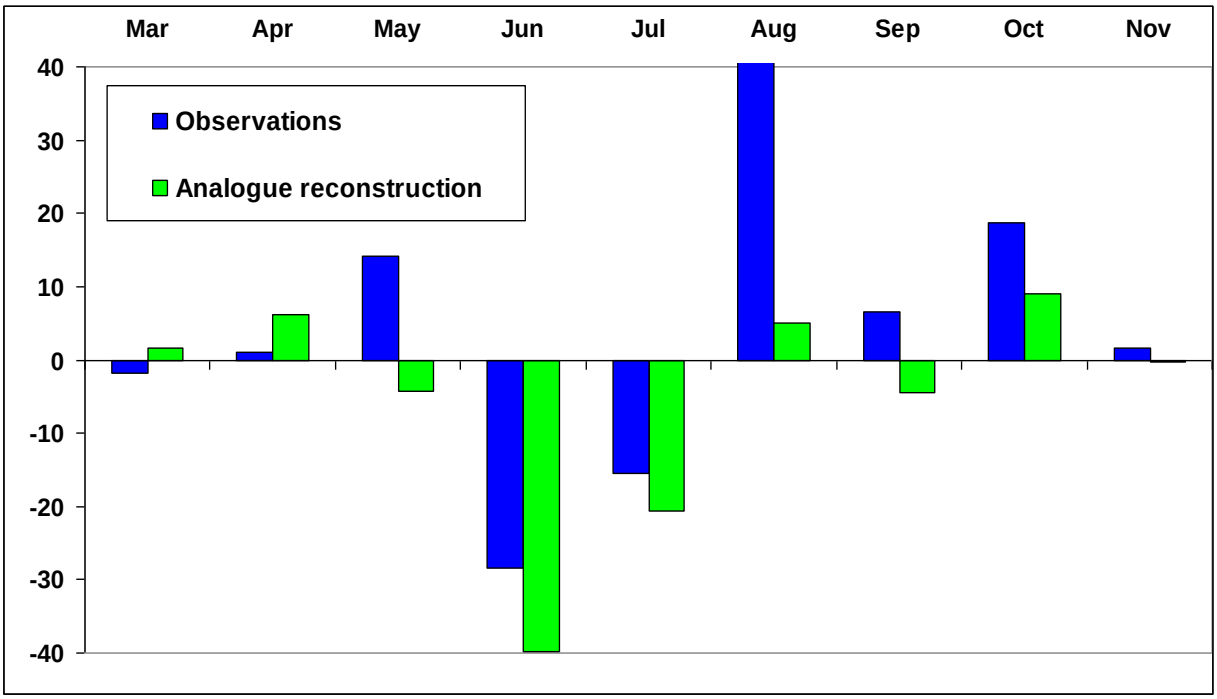

Fig 10: *Month by month linear trends from 1958 to 2006 for frost occurrences (minimum temperature below 2°C) averaged across 23 temperature stations in SEA.*

Table 9: *Spatial correlation (based on 23 stations across SEA) between linear1958 to 2006 trends for the observed series (frost occurrences and T_{min}) and analogue reconstructed series using as predictors: MSLP, MSLP combined with T_{850} and with the full optimised analogue model.*

r	MSLP only		MSLP & T_{850}		Optimised analogue	
	F. O.	$<T_{min}>$	F. O.	$<T_{min}>$	F. O.	$<T_{min}>$
Autumn	0.07	0.08	0.03	0.28	0.16	**0.40**
Winter	0.01	0.25	**0.50**	**0.60**	**0.64**	**0.64**
Spring	-0.38	-0.21	-0.06	0.01	**0.62**	**0.39**